An analytical model of off-resonant Faraday rotation in hot alkali metal vapours

Stefan L Kemp, Ifan G Hughes and Simon L Cornish

Department of Physics, University of Durham, South Road, Durham, DH1 3LE, United Kingdom

E-mail: stefan.kemp@durham.ac.uk

Abstract. We report a thorough investigation of the Faraday effect on the 852 nm D_2 transition in a hot caesium vapour, culminating in the development of a simple analytical model for off-resonant Faraday rotation. The model, applicable to all hot alkali metal vapours, is seen to predict the rotation observed in caesium, at temperatures as high as 115 °C, to within 1 % accuracy for probe light detuned by greater than 2 GHz from the D_2 lines.

Submitted to: *J. Phys. B: At. Mol. Opt. Phys.*

1. Introduction

The study of absorption and dispersion in hot alkali metal vapours is a topic of great interest. The control of these properties is exploited in, for example, slow light [1–3], light storage [4], quantum memory [5], entanglement of macroscopic systems [6], and frequency up-conversion [7]. In this work we will expand upon the flourishing interest in the Faraday effect. This phenomenon has already been put to many uses including: all-optical switching [8, 9], non-invasive atomic probing [10], far off-resonance laser locking [11], and realising a dichroic beam splitter [12].

The Faraday effect is a dispersive phenomenon manifesting itself in a frequency dependent rotation of the plane of linearly polarised light when an axial magnetic field is applied to an atomic vapour. The effect is a consequence of the circular birefringence in the medium resulting from the Zeeman shift. A significant advantage of using dispersive properties in atomic physics is that they dominate over absorption in off-resonant schemes [13]. For example, Marchant *et al.* have shown that the Faraday effect can be used to lock lasers far from atomic resonance where there is no absorption signal [11]. The motivation of this study is to characterise the off-resonant Faraday effect in a hot caesium vapour. We focus on the strong temperature dependence of the Faraday rotation signal associated primarily with the dramatic variation in the atomic vapour pressure. In particular, we present and test a simple analytical model for Faraday rotation in the off-resonant regime that can be used to predict the zero crossings of the signal, relevant to laser locking applications, and offers an improved understanding of the phenomenon.

The paper is structured as follows. In section two we outline the theory of the Faraday effect and derive a simple analytical model for the off-resonant rotation. Section three provides details on the experimental apparatus and methods. In section four we present our results on the temperature dependence of the Faraday rotation signal and test the analytical model. Finally, in section five, we summarise and conclude.

2. Theory

2.1. Faraday rotation in an atomic vapour

The absorptive and dispersive properties of a medium are encapsulated in the complex electric susceptibility, $\chi = \chi_r + i\chi_i$, where χ_r and χ_i are the real and imaginary parts of the susceptibility respectively. In a Doppler-broadened atomic vapour, χ for the transition j is given by [14]

$$\chi_j(\Delta) = c_j^2 \frac{d^2 N}{\hbar \epsilon_0} s_j(\Delta), \tag{1}$$

where c_j^2 is the transition strength, d is the reduced dipole matrix element, $\hbar$ is Planck's constant divided by 2π, ϵ_0 is the permittivity of free-space and N is the (temperature dependent) atomic number density [15]. $s_j(\Delta)$ is the lineshape of the

resonance; a convolution of the Lorentzian atomic lineshape and the Gaussian velocity distribution along the propagation direction. In the case of the D_2 transitions in the alkali metals, the total susceptibility must be calculated by summing over the allowed electric dipole transitions among the hyperfine sub-levels. From the susceptibility we can calculate the macroscopic properties of the medium: the absorption coefficient is $\alpha(\Delta) = k\,\chi_i(\Delta)$, where k is the wavenumber and Δ is the detuning; the refractive index is $\eta(\Delta) = \sqrt{\chi_r(\Delta) + 1}$. Siddons *et al.* [14] have shown that a numerical implementation of such a model leads to excellent agreement between theory and experiment for the absolute absorption profile on the rubidium D lines.

The Faraday effect arises when a magnetic field, B, is applied along the propagation direction, such that the resonant frequencies of light driving σ^+ and σ^- transitions are shifted in opposite directions by the Zeeman effect. Consequently the refractive index profiles η^+ and η^-, associated with left- and right-circularly polarised light respectively, are also shifted in opposite directions. Since the linearly polarised light incident on the vapour can be considered as a superposition of the two circular polarisations, each of these components will therefore propagate at different speeds. Upon emerging from a cell of length L there will be a relative phase between the components of $\Delta\varphi = kL\,(\eta^+ - \eta^-)$. In the case of negligible absorption, the plane of polarisation rotates by

$$\theta = \frac{kL}{2}\left(\eta^+ - \eta^-\right), \tag{2}$$

with respect to the plane of polarisation of the light incident on the cell. The model of the electric susceptibility outlined above can be used to predict accurately the Faraday rotation. However, the model can become numerically intensive as the inclusion of the Zeeman effect requires the exact diagonalisation of the full coupling Hamiltonian [12, 16]. Below we derive a simple model that is sufficient to predict accurately the extent of Faraday rotation in a far off-resonance regime.

2.2. Modelling far off-resonance Faraday rotation

When greatly detuned from an atomic resonance, dispersion increasingly dominates over absorption. It has been shown that, in this off-resonant region, the real part of the atomic lineshape factor may be approximated by

$$s_r(\Delta) \approx -1/\Delta, \tag{3}$$

where Δ is now the detuning from linecentre [13]. Combining this with equation 1, the far-detuned real susceptibility becomes

$$\chi_r(\Delta) = -c_j^2 \frac{d^2 N}{\hbar\epsilon_0 \Delta}. \tag{4}$$

Since vapour cell number densities are generally very low (χ_r is typically much less than one), we can approximate the difference between the σ^+ and σ^- refractive indices as

$$\eta^+ - \eta^- = \sqrt{\chi_r^+ + 1} - \sqrt{\chi_r^- + 1} \approx \frac{\chi_r^+ - \chi_r^-}{2}. \tag{5}$$

Again if we limit ourselves to a regime far from the atomic resonances, we may treat all of the constituent hyperfine transitions, in the single Doppler-broadened line, as a single transition of strength C^2. Furthermore we assume that the Zeeman effect translates into a shift of the refractive index profiles, η^+ and η^-, by a frequency b in opposite directions. In this case equation 5 becomes

$$\eta^+ - \eta^- = -C^2 \frac{d^2 N}{2\hbar\epsilon_0} \left[\frac{1}{\Delta + b} - \frac{1}{\Delta - b} \right]. \tag{6}$$

In the limit $|\Delta| >> b$;

$$\eta^+ - \eta^- \approx C^2 \frac{d^2 N b}{\hbar\epsilon_0 \Delta^2}. \tag{7}$$

Combining this with equation 2 the far off-resonant Faraday rotation angle is given by

$$\theta = C^2 \frac{kLd^2 N b}{2\hbar\epsilon_0 \Delta^2}. \tag{8}$$

One of the many applications of the Faraday effect is the locking of lasers at large detunings from resonance [11]. For such applications it is desirable to be able to predict the frequencies at which the zero-crossings of the Faraday rotation signal occur (*i.e.* the detunings of the locking points). Consider a set up with which locking points are generated at detunings where a rotation in the plane of polarisation of $n\pi/2$ is observed, where n is an integer. From this simple model the locking points are expected to occur at detunings

$$|\Delta_n| = \sqrt{\frac{C^2 k l d^2 b}{\pi\hbar\epsilon_0} \frac{N(T)}{n}} = \sqrt{\frac{AN(T)}{n}}, \tag{9}$$

where A is a fitting parameter characterising all the physical constants and approximations used.

3. Experimental methods

A schematic of the apparatus used to investigate the Faraday effect on the D_2 transition in caesium is shown in figure 1(a). An extended cavity diode laser at 852 nm was the light source used. The combination of a half-wave plate ($\lambda/2$), a polarisation beam splitting cube (PBS) and neutral density filters (ND) were used to create linearly polarised light of variable intensity. The probe beam then passed through a 7.5 cm heated caesium vapour cell based on the design of McCarron *et al.* [17]. An external solenoid was used to provide both heating, and an axial magnetic field if required. Upon exiting the cell, the probe passed through a second half-wave plate and the two orthogonal linearly polarised components of the beam were separated using an analysing PBS cube. These components were then focussed onto the ports of a differencing photodiode. Faraday signals were obtained by setting the analysing half-wave plate so that its optical axes were at $\pi/4$ to those of the analysing PBS cube. The output of the differencing photodiode then exhibited zero signal at detunings where the plane of polarisation was rotated by integer multiples of $\pi/2$.

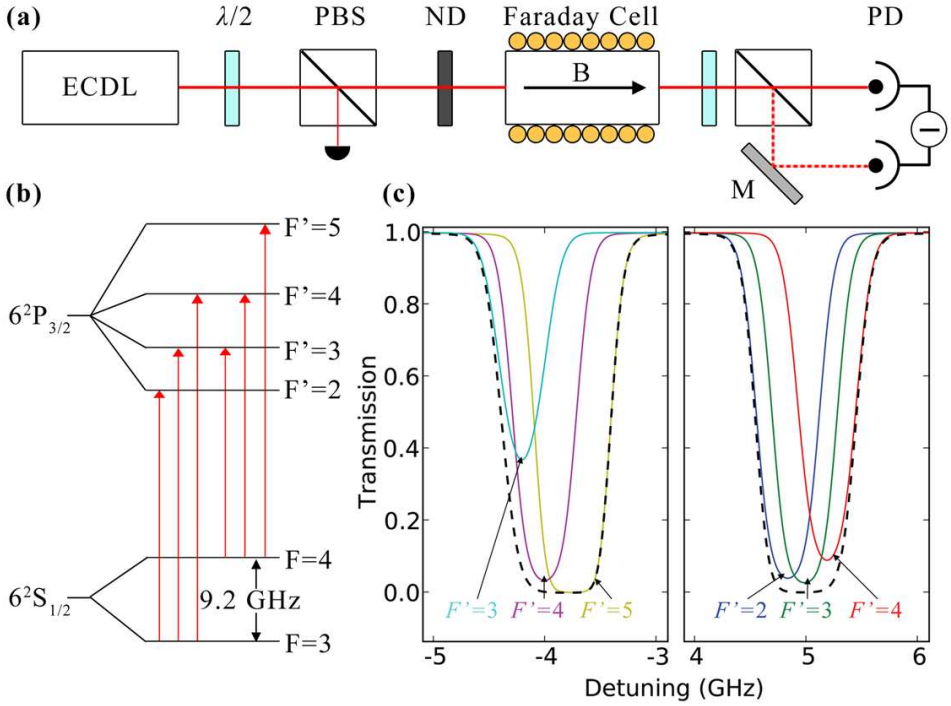

Figure 1. (a) A schematic of the experimental set up. Key: extended cavity diode laser (ECDL), half wave plate ($\lambda/2$), polarising beam splitter (PBS), neutral density filter (ND), mirror (M), and differencing photodiode (PD). (b) The hyperfine energy states and transitions that make up the D_2 lines in caesium. The excited state hyperfine splittings are approximately 251 MHz ($F' = 4$ to 5), 201 MHz (3 to 4) and 151 MHz (2 to 3). (c) The theoretical D_2 transmission in a 7.5 cm caesium vapour cell at 27 °C. The $F = 4$ line is shown on the left, and the $F = 3$ line on the right. The zero of detuning is taken to be the centre-of-mass frequency of the D_2 transition. The contributions to the absorption of each hyperfine transition are shown and labelled. The dashed black curve shows the total transmission through the cell.

The ECDL used during this experiment incorporated current feed forward circuitry which synchronised modulation of the diode current with the piezo. This allowed scan ranges of up to 12 GHz to be obtained, readily spanning both the $F = 3$ and $F = 4$ hyperfine lines (see figure 1(b) and (c)) in a single scan. Although the laser frequency scans were driven by a triangle waveform, some linearization was still required. The frequency axis of all the Faraday signals recorded for this work were linearized by simultaneously monitoring the transmission of a Fabry-Perot etalon with a free spectral range of 507 ± 1 MHz. The absolute frequency scale was established by also recording a reference spectrum from a separate saturated absorption / hyperfine pumping spectroscopy setup [18, 19] (not shown in figure 1(a)) for each Faraday signal.

The experimental method was validated by comparing the Doppler-broadened transmission of a probe beam propagating through the hot caesium vapour with the predictions of a numerical implementation of the model for the complex susceptibility following Siddons *et al.* [14]. An example theoretical spectrum is shown in figure 1(c). Measurements were taken under ambient magnetic field conditions with the

analysing half-wave plate set so that all transmitted light was incident on a single port of the differencing photodiode (the solid beam path in figure 1(a)). Spectra were recorded for both D_2 lines at a range of temperatures using the heating solenoid. These measurements allowed the identification of the weak probe regime for the beam parameters in the experiment and yielded quantitative agreement between theory and experiment to within 1 % across the full Doppler profile (see Appendix). Moreover, these measurements also allowed the thermocouple monitoring the *external* temperature of the vapour cell and solenoid to be calibrated against the *actual* temperature of the caesium vapour.

4. Results and discussion

A composite Faraday signal over the D_2 lines is shown in figure 2 for a vapour temperature of 71 °C. I_x and I_y are the intensities of the two orthogonal linear polarisations analysed by the PBS in figure 1(a), and I_0 is the intensity of the incident probe beam. For reference the absorption spectrum across the D_2 lines is shown in the sub-plot for temperatures of 71 °C (solid line) and 19 °C (dashed line). These plots reveal several interesting features of the Faraday effect. Firstly, it is worth noting that the Faraday signal is very sensitive to detuning, even in the regions where close to 100 % transmission is observed. This in itself makes the Faraday effect extremely useful since signals are produced far off-resonance without significant loss of light. Secondly, unlike rubidium, the large ground state hyperfine splitting in caesium leads to significant signal oscillation in the region between the two lines. This region should be ultra-sensitive to the distribution of atoms within the ground states. Consequently this frequency domain is a candidate for an all-optical switch [8, 9]. Finally, one notices that the region of zero Faraday signal about the linecentres of the D_2 lines does not necessarily correspond to 100 % absorption. A zero signal may be obtained with this optical set up when either the transmission of the light driving the σ^+ or σ^- transition is zero. In both cases purely circularly polarised light emerges from the cell and will result in zero differencing signal.

Faraday signals at a variety of different temperatures and axial magnetic fields have been recorded. The temperature dependence of the Faraday effect manifests itself in the relationship between the electric susceptibility and the atomic number density (see equation 1). The magnetic field dependence is due to the splitting of the hyperfine sub-levels via the Zeeman effect which displaces the refractive index profiles η^+ and η^-, associated with left- and right-circularly polarised light respectively, in opposite directions. The waterfall plots of figure 3 demonstrate the evolution of the signals with either of these variables. We can immediately see that the vapour temperature has by far the greater impact on the signals; not only do the number of zero crossings increase with increasing vapour temperature, but they also are shifted further from resonance. This sensitivity is due to the strong temperature dependence of the number density and, to a lesser extent, the width of the lineshape. Increasing the magnetic field primarily shifts the edges of the lineshapes, corresponding to the translations of the signals seen

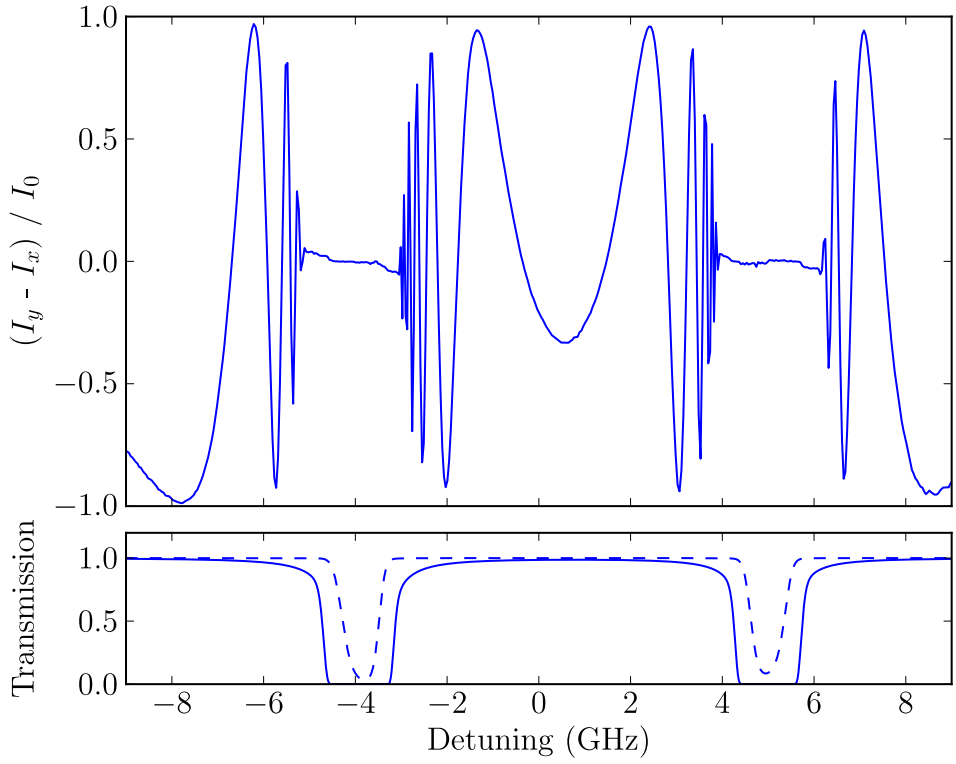

Figure 2. An example Faraday signal across the entirety of the D_2 lines at a temperature of 71 °C and a central magnetic field of 174±1 G. For comparison a transmission spectrum in the absence of the magnetic field is shown in the sub-figure for a temperature of 71 °C (solid line) and 19 °C (dashed line). The zero of detuning is taken to be the centre-of-mass frequency of the D_2 transition.

in figure 3. Additionally, there is a small increase in the frequency separations of the zero crossings as the magnetic field is increased.

In order to test the simple analytic expression (equation 9) for the far off-resonance Faraday rotation derived in section 2, we recorded the detunings of the signal zero crossings from the $F = 4$ linecentre as a function of temperature. The detunings of the first, third and seventh order zero crossings are plotted as a function of temperature in figure 4, where the order is determined by the integer n in equation 9. A fit of equation 9 to the far-detuned first order zero crossings is also included. This curve has been scaled to the other data sets by dividing by the square root of the appropriate value of n. The inset shows a Faraday signal taken at 115 °C with a central magnetic field of 117±1 G and zero crossings corresponding to the data sets on the main figure are shown. We can see from the figure that at detunings greater than 2 GHz our model works excellently, with the data points deviating from the theory by no more than 1 %. However, below 1.6 GHz there is very poor agreement with percentage deviation exceeding 30 % in some cases. This behaviour is due to the approximations used within this theory that are only valid far from resonance. In reality the lineshape is much more complicated close to resonance than the simple expression used in equation 3.

Another phenomenon observed in figure 4 is that there appears to be a temperature

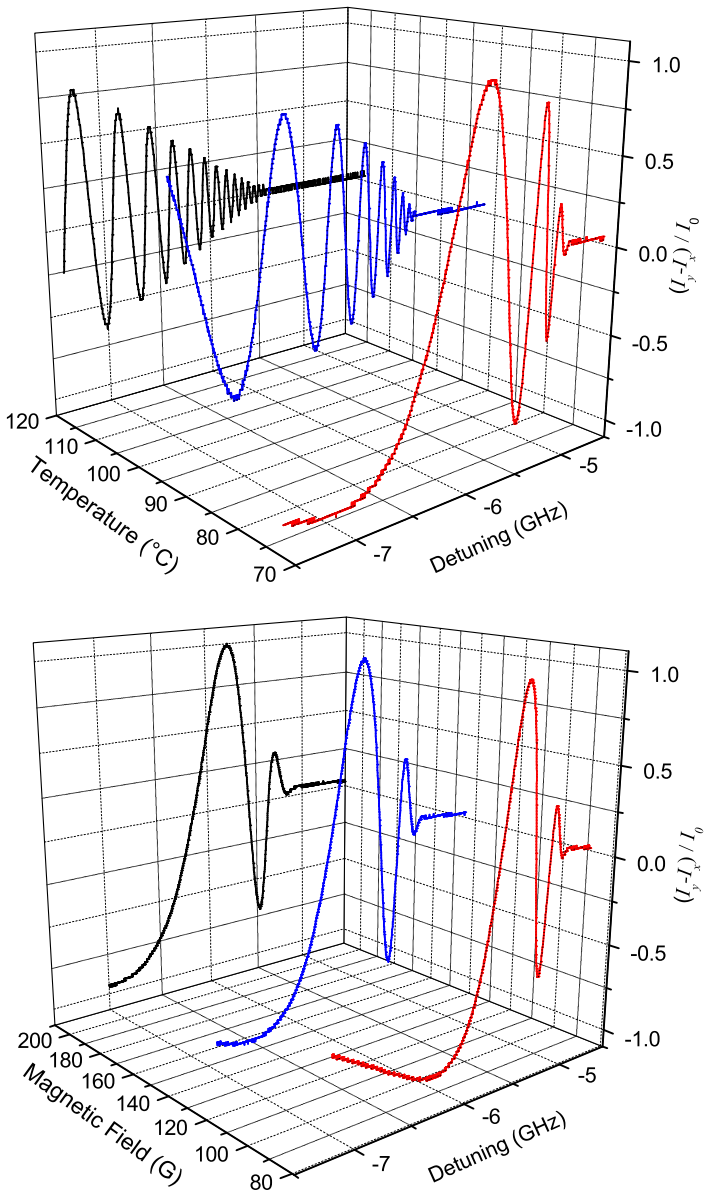

Figure 3. Top: Evolution of Faraday signals with a constant magnetic field of 117 G with temperatures of 72 °C (red), 92 °C (blue), and 116 °C (black). Bottom: Evolution of signals with a constant temperature of 61 °C and magnetic fields of 89 G (red), 145 G (blue), and 210 G (black). The zero of detuning is taken to be the centre-of-mass frequency of the D_2 transition.

dependent threshold detuning, below which there are no zero crossings. Our model fails to predict this since since it does not include the dichroism discussed earlier. The orange (light shading) region on the plot shows the region in which there is less than 5 % σ^+ transmission, and in the purple (dark shading) region there is more than 97 % transmission (calculated using the numerical implementation of the full model for the complex susceptibility). These limits are also indicated by dashed lines on the inset. This defines a window in which which zero crossings should occur. We can see from the

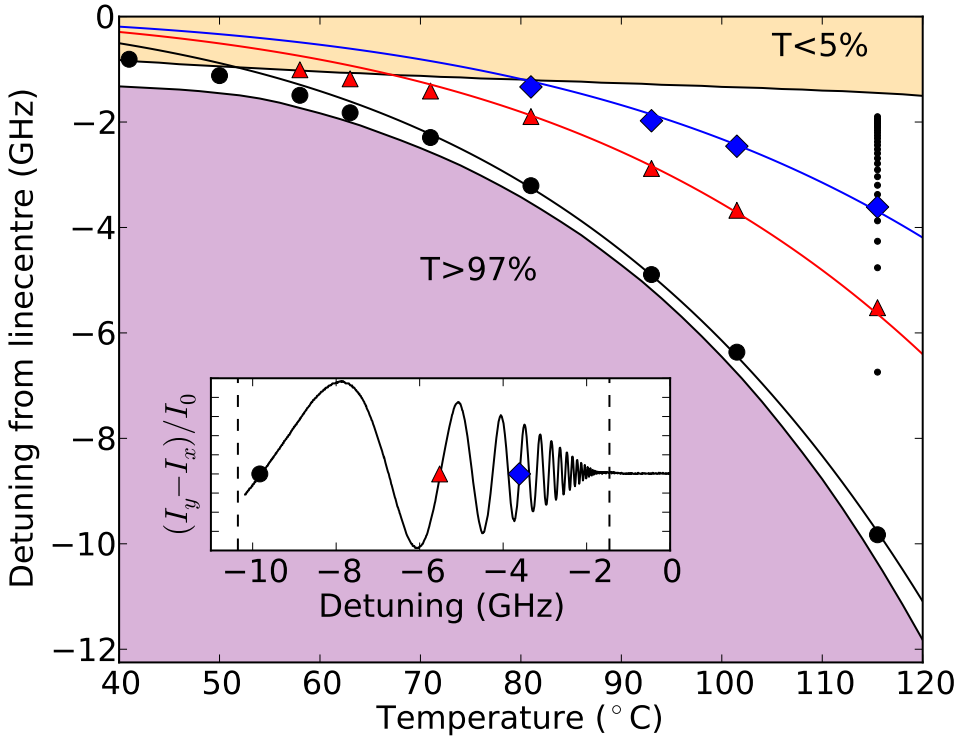

Figure 4. The red-detuning from the $F = 4$ line of the 1st (black circles), 3rd (red triangles), and 7th (blue diamonds) order zero crossings as a function of temperature for a central magnetic field of 117±1 G. The small black points indicate the locations of all discernible zero crossings on a 115 °C signal. The blue curve is a fit to our model of the 1st order crossings, the other curves are scalings of this fit. The shaded regions show the detunings at which there is less than 5 % (orange) and more than 97 % (purple) σ^+ transmission. The inset shows the signal recorded at 115 °C and the locations of the various zero crossings.

figure that it is indeed the case that no zero crossings occur outside this white region.

This simple model works exceptionally well at large detunings, which is the region it was designed to describe and where the off-resonant Faraday effect is likely to find the most use. This approximation can be used as a quick calibration tool for an inexpensive and simple method of locking lasers far from resonance; a necessity in some optical dipole trapping schemes. In addition to the results presented here, which has focussed on red-detuned light from the $F = 4$ line, we have verified that this model is successful at other magnetic field strengths for both lines. We have also used the model to successfully predict locking points in the rubidium D_2 lines by fitting to the data presented by Marchant *et al.* [11].

5. Conclusion

In summary we have developed a simple model that predicts the Faraday rotation at large detunings from resonance for the D_2 transitions in caesium and rubidium. This model has been demonstrated to be accurate to within 1 % of experimental data, at

detunings greater than 2 GHz from resonance, for temperatures up to 115 °C. The major advantage of this model is that only a single Faraday signal is required for calibration. The zero crossings of other Faraday signals for different temperatures may then be extrapolated from a fit to the model. Consequently this model has potential as a calibration technique for applications which exploit the zero crossings of the Faraday signal as a simple and inexpensive method of laser frequency stabilization far from resonance.

Acknowledgments

We are grateful to P. Siddons and L. Weller for assistance in adapting the susceptibility code from rubidium to caesium, and C.S. Adams for carefully reading the manuscript.

Appendix. Absolute absorption and the weak probe regime

All of the measurements reported in this manuscript were performed in the weak probe regime where the intensity of the light is sufficiently low that the change in the atomic populations in the sample is negligible. To establish this regime for the beam parameters used in the experiment, the linecentre transmission of both the $F = 3$ and $F = 4$ lines was recorded across a large range of probe intensities. The results of this study are presented in figure 5. Included in this plot are lines to guide the eye, which model the absorption coefficient as

$$\alpha = \alpha_{\text{weak}} \left(1 + \beta \frac{I}{I_{\text{sat}}}\right)^{-1/2}, \tag{10}$$

where α_{weak} is the theoretical value of α in the weak probe regime. β is a fitting parameter characterising the change in the saturation intensity due to hyperfine pumping[20]. It is immediately apparent from this plot that, at intensities below $0.01\, I_{\text{sat}}$ (where the saturation intensity is $I_{\text{sat}} = 2.7\,\text{mW}\,\text{cm}^{-2}$ [21]) , the experimental transmission converges to the theoretical value. It is also evident that for higher intensities the $F = 4$ transition is less strongly affected by hyperfine pumping due to the dominance of the closed $F = 4 \rightarrow F' = 5$ transition (see figure 1(c)). The insets to figure 5 show the transmission across each line at temperatures of 20 °C (top curves), 25 °C (middle) and 47 °C (bottom)at 19 °C for a probe intensity of $0.001\, I_{\text{sat}}$. The dashed black curves show the theoretical transmission calculated using a numerical implementation of the model for the complex susceptibility following Siddons *et al.* [14]. It is clear to see that there is excellent agreement between theory and experiment across both of the D_2 lines; the rms deviation is below 1 %. Such careful comparisons of theory and experiment were used to provide a calibration of the temperature of the caesium vapour within the cell and solenoid.

References

[1] Fleischhauer M, Imamoglu A and Marangos J P 2005 *Rev. Mod. Phys.* **77** 633

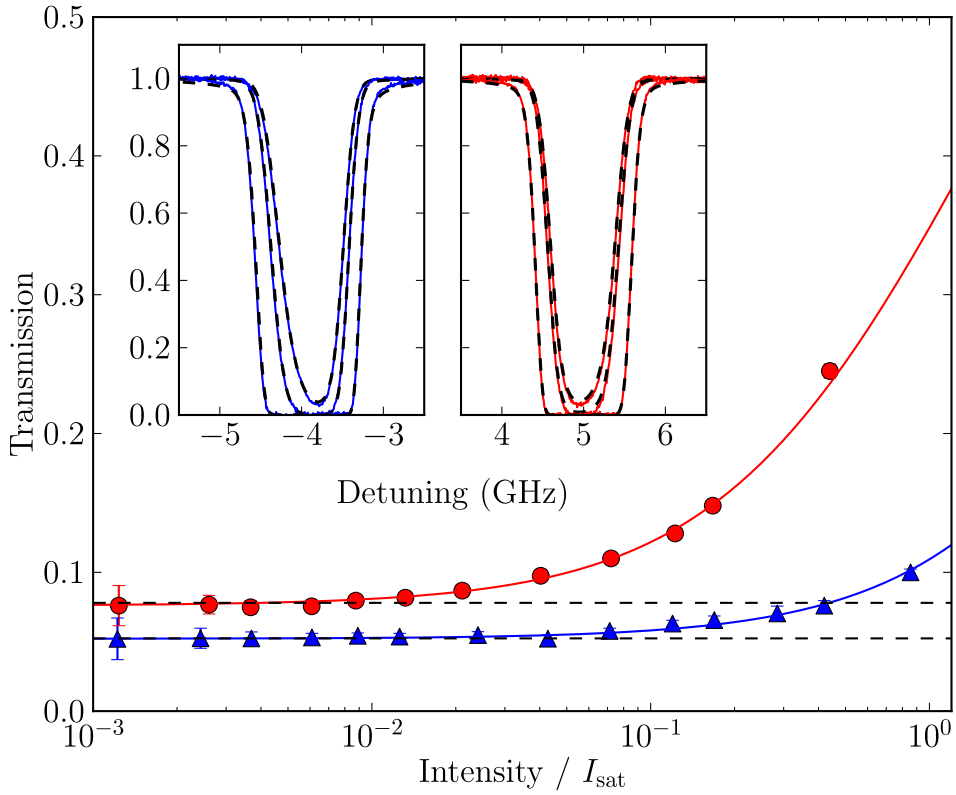

Figure 5. Linecentre transmission as a function of probe intensity for the $F = 3$ (red circles) and $F = 4$ (blue triangles) lines. The corresponding curves are fits to equation 10. The horizontal dashed black lines show the theoretical transmission in the weak probe regime for each line. The insets show the transmission across each line at temperatures of 20 °C (top curves), 25 °C (middle) and 47 °C (bottom) for a probe intensity of 0.001 I_{sat}. The dashed black curves show the theoretical transmission. The zero of detuning is taken to be the centre-of-mass frequency of the D_2 transition.

[2] Khurgin J B 2010 *Adv. Opt. Photon.* **2** 287
[3] Milonni P W 2002 *J. Phys. B: At. Mol. Opt. Phys.* **35** R31
[4] Phillips D F, Fleischhauer A, Mair A, Walsworth R L and Lukin M D 2001 *Phys. Rev. Lett.* **86** 783
[5] Julsgaard B, Sherson J, Cirac J I, Fiurášek J and Polzik E S 2004 *Nature* **432** 482
[6] Jensen K *et al.* 2011 *Nat. Phys.* **7** 13
[7] Vernier A, Franke-Arnold S, Riis E and Arnold A S 2010 *Opt. Express* **18** 17020
[8] Dawes A, Illing L, Greenberg J and Gauthier D 2008 *Phys. Rev. A* **77** 013833
[9] Siddons P, Adams C S and Hughes I G 2010 *Phys. Rev. A* **81** 043838
[10] Siddons P, Bell N C, Cai Y, Adams C S and Hughes I G 2009 *Nat. Photon.* **3** 225
[11] Marchant A L, Händel S, Wiles T P, Hopkins S A, Adams C S and Cornish S L 2011 *Opt. Lett.* **36** 64
[12] Abel R P, Krohn U, Siddons P, Hughes I G and Adams C S 2009 *Opt. Lett.* **34** 3071
[13] Siddons P, Adams C S and Hughes I G 2009 *J. Phys. B: At. Mol. Opt. Phys.* **42** 175004
[14] Siddons P, Adams C S, Ge C and Hughes I G 2008 *J. Phys. B: At. Mol. Opt. Phys.* **41** 155004
[15] Alcock C B, Itkin V P and Horrigan M K 1984 *Canadian Metallurgical Quarterly* **23** 309
[16] Popescu A, Schorstein K and Walther T 2004 *Appl. Phys. B* **79** 955
[17] McCarron D J, Hughes I G, Tierney P and Cornish S L 2007 *Rev. Sci. Instrum.* **78** 093106
[18] MacAdam K B, Steinbach A and Wieman C 1992 *Am. J. Phys.* **60** 1098

[19] Smith D A and Hughes I G 2004 *Am. J. Phys.* **72** 631
[20] Sherlock B E and Hughes I G 2009 *Am. J. Phys.* **77** 111
[21] Corney A 1977 *Atomic and Laser Spectroscopy* (Oxford: Oxford University Press)